ELSEVIER

Biochimica et Biophysica Acta 1370 (1998) 127–137

BIOCHIMICA ET BIOPHYSICA ACTA
BBA

Surface behavior of myelin monolayers

Rafael G. Oliveira, Reyna O. Calderón, Bruno Maggio *

Departamento de Química Biológica-CIQUIBIC, Facultad de Ciencias Químicas, Universidad Nacional de Córdoba, Ag. Postal 4, CC 61, 5000 Córdoba, Argentina

Received 26 August 1997; revised 17 October 1997; accepted 24 October 1997

Abstract

Myelin can be spread as a stable monomolecular layer, with reproducible properties, at the air–water interface. The major lipids and proteins of myelin are represented in this monolayer in molar ratios similar to those in the original membrane. A well-defined collapse point of the myelin monolayer occurs at ca. 46 mN/m. At a surface pressure of ca. 20 mN/m, the surface pressure–molecular area isotherm of the myelin monolayer shows a change in its compressibility, exhibited as a diffuse but reproducible inflection with a clearly marked change of the surface compressional modulus; the surface potential–area curve shows a change of slope at the same surface pressure. The myelin monolayer shows considerable hysteresis during the first compression–decompression cycle; no detectable protein unfolding under expansion; and decreased hysteresis after the first cycle. The average molecular areas, the inflection at 20 mN/m, the variation of the surface potential per unit of molecular surface density, and the hysteresis properties of the myelin monolayer indicate that this membrane undergoes changes of intermolecular organization mostly ascribed to the protein fraction, above a lateral surface pressure of ca. 20 mN/m. The behavior is consistent with a surface pressure-dependent relocation of protein components in the film. This has marked effects on the stability, molecular packing, and dipolar organization of the myelin interface. © 1998 Elsevier Science B.V.

Keywords: Myelin; Monolayer; Hysteresis; Biomembrane monolayer

1. Introduction

Monomolecular layers (monolayers) at the air–water interface have been widely used in order to study properties of purified membrane components and their simple mixtures under controlled intermolecular organization [1,2]. On the other hand, pioneering work regarding formation of monolayers from vesiculated lipid bilayers and from vesicles of whole-cell membranes was described many years ago [3,4]. More recently, we carried out the preparation and characterization of a monomolecular layer prepared from a plasma membrane of neuronal origin using a highly purified axolemma subcellular fraction [5,6]. In addition, planar supported films, derived from this monolayer, were used to study the biological response of Schwann cells cultured upon the supported axolemma monolayer with different well-defined intermolecular organizations. The Schwann cell response was reflected by changes in proliferation, shape, growth pattern, and in the differential exposure of surface antigens, depending on the surface organization of axolemma [6].

In this work, we have characterized the surface behavior of a monomolecular layer prepared from

* Corresponding author. Fax: 54-51-334074.

PII S0005-2736(97)00254-X

central nervous system myelin, the typical differentiated plasma membrane of oligodendroglial origin.

2. Materials and methods

2.1. Myelin vesicles and lipids

Highly purified myelin was prepared from bovine spinal cord [7]. Myelin vesiculation was carried out using the method of Wutrich and Steck [8]. Briefly, one volume of packed myelin was gently dispersed in 100 volumes of phosphate buffer saline 1 mM, pH 8, containing 2 mg/ml dithiotreitol and gently stirred at 4°C for 18 h. The suspension was centrifuged at 25 000 × *g* for 30 min.The pellet was resuspended in the same buffer to a final protein concentration of 0.24 mg/ml, and passed five times through a 26 G needle fitted to a glass syringe. Vesiculation was ensured by entrapment of 25 mM carboxyfluorescein and measurement of its fluorescence enhancement by dilution dequenching after adding Na-deoxycholate (1% final concentration) to the myelin vesicles in a spectrofluorometer cuvette while stirring [5,9].

Total lipids from whole myelin, or from monolayers collected as indicated below, were extracted and partitioned as described previously [10]. The lower phase after Folch's partition was dried under nitrogen and redissolved in chloroform–methanol (2 : 1). Phospholipid phosphorous was measured by the modified micro-procedure of Bartlett [11]. For individual lipid analysis, 12 μg of total lipids were analyzed by HPTLC developed with chloroform–methanol–water (70 : 30 : 4) as described by Coetzee et al. [12]. Individual lipids were visualized with Cu-acetate reagent [13] and quantified by scanning densitometry (Shimadzu CS-930 densitometer, Shimadzu, Japan). Standard curves of purified lipid standards were run on the same plate as the samples and calibration curves were constructed for each major myelin lipid species [13]. Cholesterol was determined enzymatically with a commercial kit (GT Laboratorios, Argentina).

Sodium dodecyl sulfate polyacrylamide gel electrophoresis (SDS-PAGE) was performed on ca. 1 μg of protein from myelin vesicles or from collected monolayers. The material from the monolayer (and, as a control for recovery assays, from myelin vesicles that were diluted to the same final concentration as the film material) was concentrated by ultrafiltration (Centriprep-10 concentrators, Amicon, Beverly, MA). The concentrated samples were layered onto 13% polyacrylamide (stacking gel was 4% polyacrylamide) according to Laemmli [14]. Protein standards were simultaneously separated on the same gel slab. Visualization was performed with a silver stain procedure [15]. The molecular weights of the major protein bands were ascribed after calibration with molecular weight markers. The relative amounts of individual bands were determined by densitometry (Shimadzu CS-930 densitometer, Shimadzu, Japan). Absolute amounts of proteins were determined by the method of Lowry [16] in the presence of 0.2% sodium dodecyl sulfate using bovine serum albumin as standard.

2.2. Preparation of myelin monolayers

Myelin vesicles were spread at the air–water interface, as described before for axolemma [5]. In brief, the vesicles (0.24 mg protein/ml) were allowed to flow down (approximate rate 10 μl/min) a 5 mm diameter wetted glass rod positioned at an angle of 45° across the aqueous surface in a compartment (80 ml) of a specially designed thermostated Teflon-coated trough, with multiple compartments, filled with 10 mM Tris[hydroxymethyl]aminomethane buffer in 100 mM NaCl, 20 mM $CaCl_2$, adjusted to pH 7.4 with HCl. Monolayers from the extracted lipid fraction were spread directly from their chloroform-methanol (2 : 1) solutions [17]. The temperature was maintained at 25 ± 2°C. A 12 μl aliquot of vesicle suspension or of purified lipid fraction (10–17 nmol lipid) were spread onto a surface of 80 cm^2. The surface pressure (Wilhelmy method via platinized-Pt plate), the area enclosing the monolayer, and the surface potential (via millivoltmeter with air-ionizing ^{241}Am plate and calomel electrode pair) were automatically measured (with the control unit Monofilmmeter with Film Lift, Mayer Feintechnique, Gottingen, Germany) and recorded continuously and simultaneously with a double channel X-Y-Y recorder. The spreading rate of the vesiculated myelin membrane against a constant surface pressure of 2 mN/m was 33 ± 3 cm^2/min, similar to that of other membranes [5,18].

In order to collect the monolayers, vesicles were spread on the surface of a trough compartment communicated by a narrow and shallow slit with another compartment filled with fresh buffer. After spreading, the film was free-energy-shocked by sudden expansion to twice the initial area. This causes further spreading of residual vesicles adsorbed to the interface [5,18]. Subsequently, the film was washed by transferring it over a compartment with fresh buffer, checking that the area covered by the film at collapse was that expected from the known amount of material initially spread on the basis of the previously obtained surface pressure–molecular area isotherm. The film transfer eliminates membranous material that would not spread or that remained loosely associated to the interface [5,19].

For protein and lipid analysis, about 70 monolayers were recovered by aspiration into a small glass vial fitted with a 25 G needle and a suction outlet. The monolayers were recovered in the collapsed state since this resulted in the collection of a lower amount of subphase which simplifies the subsequent concentration step. The complete aspiration of the monolayer was directly ascertained by the decay of the surface pressure to zero, measured at the surface of the compartment over which collection was done. Similar results were obtained with washed monolayers collected at surface pressures between 10–20 mN/m; however, in these conditions the amount of subphase volume collected was unavoidably large and this complicated the concentration step.

The surface behavior of the monolayer was characterized by recording isothermally, at 25 ± 2°C, the following: surface pressure, surface potential, surface potential normalized per unit of molecular surface density (usually denominated surface potential/molecule [20–22]) as functions of the molecular area, and by the adsorption isotherm (surface pressure as a function of time, at constant area). The routine compression rate was ca. 41 cm^2/min, no significant differences were obtained between compression rates from 24 cm^2/min up to 104 cm^2/min. The mean molecular area, surface pressure, and surface potential in different independent experiments were within ± 0.015 nm^2, ± 1 mN/m and ± 10 mV. Reproducibility of the limiting molecular area of the surface pressure– and surface potential–molecular area isotherms under expansion and recompression cycles indicates that no further material is lost or incorporated into the monolayer. The expansion and recom-

Table 1
Membrane recovery and lipid distribution [a]

	Vesicles	Spread monolayer	Yield (%) [b]
Protein (μg)	2.88	1.56	54.0
Total Lipids (μg)	9.57	5.66	59.1
Total Phospholipids (nmol)	6.20	3.52	56.8

	Vesicles			Spread monolayer		
	μmol/mg protein	%total lipid	Phosph.	μmol/mg protein	%total lipid	%Phosph.
Total phospholipid	2.15	42	100	2.26	38	100
SPM	0.46		21.4	0.54		23.7
PC	0.36		16.6	0.42		18.4
PE	1.02		47.6	0.89		39.4
PS	0.31		14.2	0.42		18.4
Cholesterol	1.89	37		2.49	42	
Cerebrosides	0.82	16		0.89	15	
Sulfatides	0.26	5		0.18	3	
Chol/phosph	0.88			1.11		

[a] Among different experiments, maximum SEM was ±3% for proteins, ±11% for total and individual lipids, with respect to the average values given above. Abbreviations: SPM, sphingomyelin; PC, phosphatidylcholine; PE, phosphatidylethanolamine; PS, phosphatidylserine; Chol., cholesterol; Phosph., total phospholipid.

[b] The column labelled ''Yield'' is the amount of material recovered from the monolayer with respect to that present in the amount of vesicles spread (taken as 100%), and represents a mean over 70 films collected.

pression cycles also provide information on the hysteresis properties of myelin.

The average molecular area of myelin monolayers was calculated from the mole fraction of the major lipid and protein fractions present in the monolayer (Table 1) determined as described above. Number-averaged molecular weight [23] of the total lipid and protein fraction mixtures (628 Da and 25.00 kDa, respectively) were used to obtain the mean number of molecules at the surface. The features contributed by the total protein fraction to those of the myelin film can be directly calculated from the known isotherms of whole myelin and that of the total lipid fraction [5–20]. The surface behavior of the total protein fraction was obtained, at each surface pressure, according to Eqs. (1)–(3):

$$A_{\mathrm{P}}]_{\Pi} = \frac{A_{\mathrm{M}}]_{\Pi} - A_{\mathrm{L}}]_{\Pi} \times X_{\mathrm{L}}}{X_{\mathrm{P}}} \quad (1)$$

$$\Delta V/n_{\mathrm{P}}]_{\Pi} = \frac{\Delta V/n_{\mathrm{M}}]_{\Pi} - \Delta V/n_{\mathrm{L}}]_{\Pi} \times X_{\mathrm{L}}}{X_{\mathrm{P}}} \quad (2)$$

$$\Delta V_{\mathrm{P}}]_{\Pi} = \Delta V/n_{\mathrm{P}}]_{\Pi} \times A_{\mathrm{P}}]_{\Pi} \quad (3)$$

where, taken at a constant surface pressure Π, $A_{\mathrm{P}}]_{\Pi}$ is the mean molecular area of the total protein fraction; $A_{\mathrm{M}}]_{\Pi}$ the mean molecular area of the total myelin film, $A_{\mathrm{L}}]_{\Pi}$ the mean molecular area of the total lipid fraction, $\Delta V/n_{\mathrm{P}}]_{\Pi}$ the mean surface potential/molecule of the total protein fraction, $\Delta V/\mathrm{n}_{\mathrm{M}}]_{\Pi}$ the mean surface potential/molecule of the total myelin film, $\Delta V/n_{\mathrm{L}}]_{\Pi}$ the mean surface potential/molecule of the total lipid fraction, $\Delta V_{\mathrm{P}}]_{\Pi}$ the mean surface potential of the total protein fraction, and X is the corresponding mole fraction of the total protein and total lipid components in the monolayer.

3. Results and discussion

3.1. Yield of myelin membrane material in the monolayer

The recovery of proteins in the myelin monolayer represents a yield of 54% with respect to the amount of protein present in the aliquot of membrane vesicle suspension spread onto the surface (Table 1). Total phospholipid spread with a similar yield of 56.8%. Thus, similar to what was previously found for axolemma [5], the phospholipid/protein ratio present in myelin vesicles is maintained when the membrane was spread as a monolayer.

All lipid species found in the myelin monolayer are represented at comparable mole fractions to those in the original myelin vesicle preparation (Table 1). Compared to the yield of 26.6%, previously reported for axolemma monolayers [5], the recovery of total phospholipids in the myelin monolayer is higher. Similar to axolemma, PE is moderately depleted in the myelin monolayer while PS and cholesterol are slightly increased, and the myelin monolayer contains the entire range of protein species present in the vesicle membrane (Fig. 1). The high molecular weight material at the top of the gel in lane 1 (monolayer) and 2 (ultrafiltrated vesicles) in Fig. 1 is probably due to some protein aggregation [24] occurring during the sample concentration step by ultrafiltration; myelin vesicles that were not submitted to concentration (lane 3) do not show aggregation.

3.2. Surface behavior of monolayers from the total lipid fraction

Fig. 2(a) shows the surface pressure, the surface potential and the surface potential/molecule of the

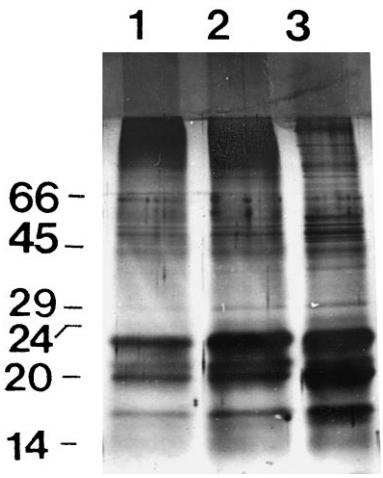

Fig. 1. SDS-PAGE of myelin vesicles and myelin monolayers. Numbers on the left show position of molecular weight markers. Lane 1 – myelin monolayer; lane 2 – myelin vesicles concentrated by ultrafiltration; and lane 3 – myelin vesicles not concentrated.

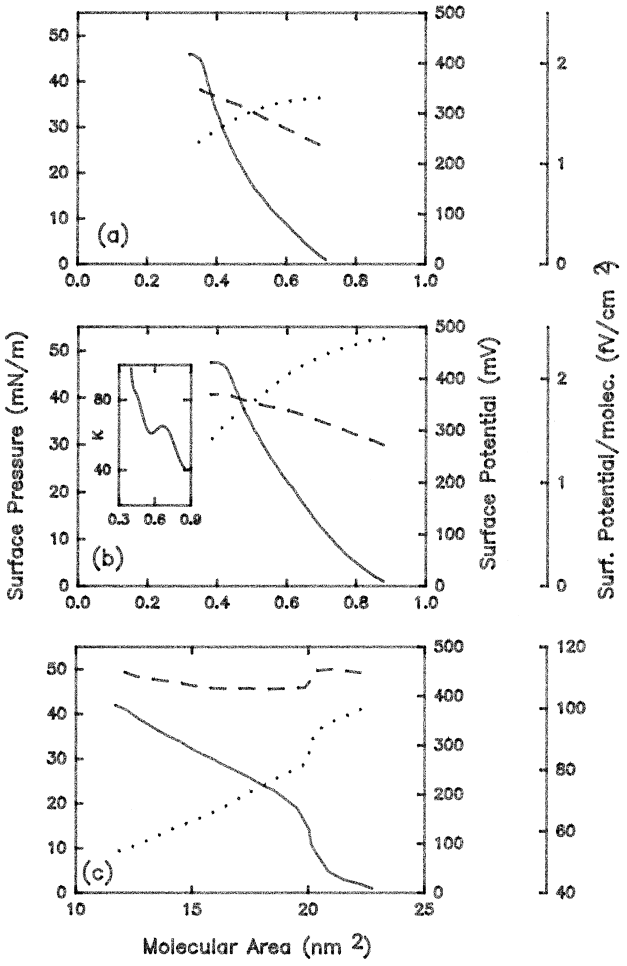

Fig. 2. Compression isotherms of myelin. The variation of the surface pressure (————), surface potential (---) and surface potential/molecule (· · ·) as a function of the mean molecular area. (a) – lipid fraction; (b) – total myelin; and (c) – calculated isotherms for the total protein fraction. No further increases of surface pressure were observed above the plateau pressure point, even after reducing the film area to one third of the limiting molecular area for both the lipid fraction and whole myelin monolayer. The inset in (b) represents the variation of the surface compressional modulus [K (mN/m)] as a function of the mean molecular area of the myelin monolayer.

total lipid fraction from the lower phase of Folch's partition performed on the material collected from the monolayer, similar curves were obtained for the total lipid fraction extracted from the original myelin vesicles. The isotherm in Fig. 2(a) shows a compression behavior that is characteristic of an expanded liquid state, with a collapse pressure point and an equilibrium spreading pressure of 42–44 mN/m, limiting molecular area of 0.365 nm^2 and maximum surface potential of 343 mV and 1.25 fV cm^2/molecule. The surface pressure–molecular area isotherm of the total lipid fraction from myelin is more condensed than that derived from axolemma [5]. A smooth gradual decrease of the surface potential/molecule is observed under compression that is comparable to that found for the total lipid fraction of axolemma [5]. This type of variation, common to several lipids, indicates little reorientation or relocation of dipolar components during changes in packing [22].

3.3. Surface behavior of whole myelin monolayers and the total protein fraction

The compression isotherm of the myelin monolayer is shown in Fig. 2(b). The isotherm of whole myelin is displaced to larger mean molecular areas, it is more compressible, and the surface potential reaches slightly higher values (367 mV) at a higher collapse pressure point than that of the lipid fraction. The myelin monolayer shows a change of compressibility in the surface pressure–molecular area isotherm occurring at ca. 20 mN/m and a molecular area of ca. 60–65 nm^2, clearly emphasized by the variation of the surface compressional modulus with the mean molecular area (see inset in Fig. 2(b)). The values of the compressional modulus correspond to a liquid interface [25], exhibiting a transition between a more expanded to a more condensed state. The variation in the compressional modulus is also reflected as a change in the slope of the surface potential–molecular area curve occurring at the same molecular area (Fig. 2(b), dashed line). Also, a marked inflection occurring above about 20 mN/m is clearly apparent in the adsorption isotherm (Fig. 3). Compared to axolemma [5], the isotherm of the myelin monolayer is more similar to that exhibited by the total lipid fraction, it is displaced to smaller mean molecular areas at all surface pressures and it is more condensed as indicated by its higher compressional modulus at all molecular areas. This might have been expected on the basis of the lower content in proteins of myelin; on a weight basis, the lipid/protein ratio is 3.63 in the myelin monolayer (see Table 1) compared to 0.99 in axolemma [5].

The equilibrium spreading pressure (pressure point at which bulk phase myelin and spread monolayer are

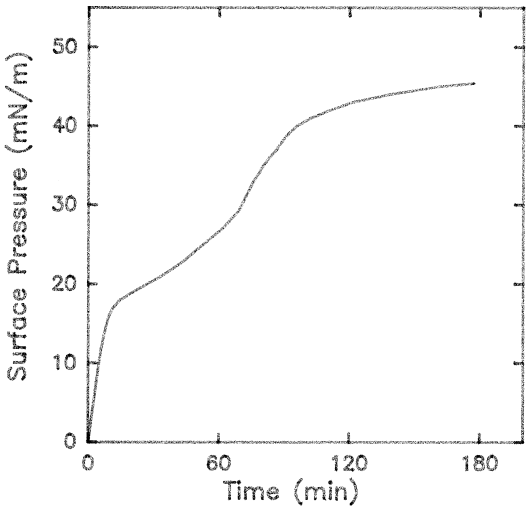

Fig. 3. Adsorption isotherm of total myelin. Myelin vesicles (2.4 mg protein) were injected into a stirred compartment (subphase 18 ml and surface area 18 cm^2).

in equilibrium) of the myelin monolayer is between 45–47 mN/m, as determined by depositing excess material at the interface and following the surface pressure variation with time. Within experimental error this is comparable to the collapse pressure point (46 mN/m), which represents a surface pressure point at which two different structural phases, the monolayer and the collapsed phase coexist [1,20]. If the film compression was stopped at the collapse point, the surface pressure remained constant (within ± 1 mN/m) with time. Also, the collapse pressure coincides with the maximum surface pressure of ca. 46 mN/m attainable by spontaneous formation of a monolayer from the adsorption and spreading of material from vesicles injected into the subphase (Fig. 3), or from myelin dissolved in chloroform–methanol (2 : 1) (see below). For monolayers in the liquid state the equilibrium spreading pressure is the same as the collapse pressure [20,26]. It has long been shown that the mesomorphic state of myelin at room temperature corresponds to that of a liquid-crystalline phase [27] in which its membrane components exhibit a lateral mobility similar to that observed in other fluid membranes [28]. The similarity between myelin collapse pressure and equilibrium spreading pressure supports the fact that the monolayer is in the liquid state at the temperature used in our studies; this is also revealed by the values of the surface compressional modulus [25]. Our observations suggest that myelin can exist at high surface pressures in a state of stable equilibrium between at least two different interfacial arrangements, a closely packed monolayer state and the collapsed bulk (usually multilayered [1,20]) phase (see Section 3.4).

Wet myelin dissolves completely in 19 volumes of chloroform–methanol (2 : 1) [29], although some of its high molecular weight protein components (mostly Wolfgram proteins) tend to aggregate when this solution is left to stand for a period of time [30]. Freshly dissolved myelin in chloroform–methanol (2 : 1), immediately spread from this solution, gave the same isotherm (with the same limiting molecular area, surface potential, and collapse pressure) as that obtained by spreading the aqueous suspension of vesicles as described in Section 2. This is indicative that the surface free energy shock of the vesicles during the spreading procedure results in the same surface organization as when the components reorganize at the surface from their solution in organic solvent; it also shows that the interfacial intermolecular organization acquired in the myelin film is very stable (see below) since it is independent of the initial physical state of the material spread. This is similar to other protein [31] and lipid-protein systems [32], in which the isotherms of monolayers spread from different organic solvents and aqueous dispersions (vesicles in the case of lipid–protein systems) lead to a similar final interfacial behavior [33]. Also, apart from the reproducible limiting molecular areas under successive compression–expansion cycles mentioned above, the similarity between the isotherms spread from vesicles or from the organic solvent solution indicates that there is no further spreading from vesicles after the surface free energy shock (see Section 2) since vesicles are not present in the chloroform–methanol solution of myelin. If the latter solution was not spread immediately after preparing, the isotherms become progressively different and irreproducible, probably due to a slow aggregation of protein components that can be visually observed in the organic solvent.

On the basis of the measured lipid and protein mole fractions in the myelin monolayer, the surface behavior contributed by the total protein fraction was directly calculated from the known isotherms of total

myelin and the total lipid fraction as described in Section 2. The surface pressure–surface potential/molecule-area isotherms of the protein fraction clearly emphasize, as a marked discontinuity, the change in compressibility and variation of the surface potential/molecule shown at ca. 20 mN/m in the isotherm of whole myelin (see Fig. 2(c)). The isotherm corresponding to the total protein fraction indicates a compressibility characteristic of liquid-expanded protein monolayers [31]. At ca. 20 mN/m and a molecular area of ca. 20 nm^2, a rather abrupt change of intermolecular organization occurs. This is also reflected by a considerable reorientation and/or relocation of overall protein molecular dipoles (measured in the direction perpendicular to the surface [20–22]) as indicated by the marked step in the surface potential/molecule-area curve. The changes occurring in the resultant dipoles of the protein fraction in the myelin monolayer under compression are more abrupt than in axolemma [5]. Above 20 mN/m, the monolayer of the total protein fraction of myelin shows no further change of surface potential and a constant compressibility. A wide variety of protein monolayers including myelin basic proteins [31], and Folch's proteolipid [34] show collapse pressure points near 20 mN/m; further compression of these protein monolayers beyond this pressure leads to essentially linear increases of the surface pressure and no additional changes of surface potential and compressibility [31,33].

3.4. Hysteresis and stability of myelin monolayers

Although little studied, the occurrence of hysteresis under successive compression and decompression cycles is a common phenomena in monolayers at the aqueous–air interface [1,35,36]. These effects arise from a balance among cohesion phenomena and viscoelastic properties of the interface that have different reversibility properties. In essence, these phenomena indicate that different molecular arrangements can be obtained depending on whether the energy and kinetic barriers for intermolecular cohesion are different to those involved in the hydrophilic–hydrophobic balance and polar head group–subphase interaction that determine molecular dispersion through interfacial spreading [1,36]. Thus, the presence of hysteresis is related to the stability of closely packed liquid-condensed states formed under compression and their tendency to undergo reversible reorganization to their initial liquid-expanded states under expansion, during the time of the experiment (Carrer and Maggio, unpublished results).

Fig. 4 shows that initially, both the monolayer from the total lipid fraction (Fig. 4(a)) and that from whole myelin (Fig. 4(b)) exhibit considerable hysteresis. In the first compression–decompression cycle the free energy change involved in the compression process is different to that released during expansion for both total lipid and whole myelin monolayers. This is reflected in the $\Delta\Delta G$ values in Table 2. This magnitude is indicative of the energy trapped (as viscoelastic effects and/or cohesive intra- or inter-

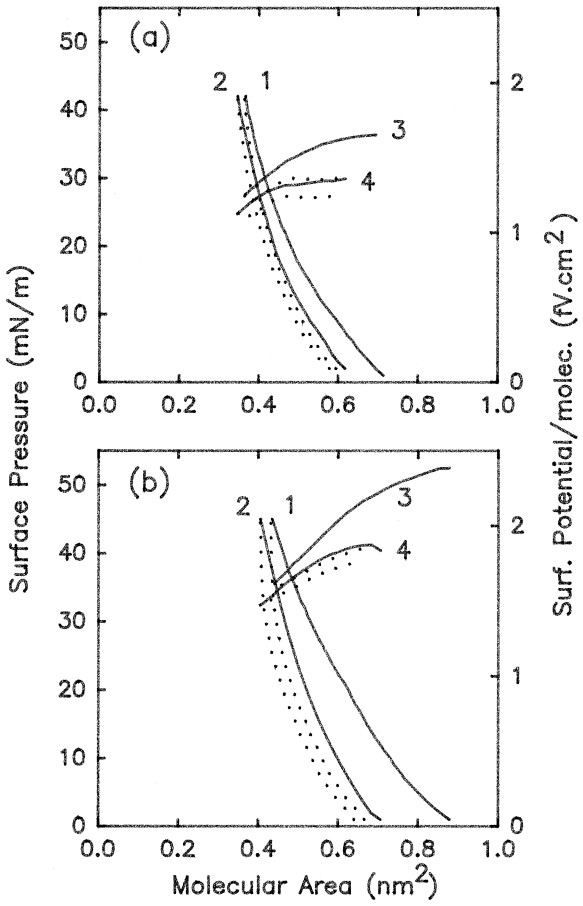

Fig. 4. Hysteresis cycles in myelin. Compression (————) and expansion (· · ·) behavior of the (a) total lipid fraction and (b) myelin monolayers in the (1) first and (2) second cycles for the surface pressure-area isotherm and in the (3) first and (4) second cycles for the surface potential/molecule-area isotherm.

Table 2
Free energy of compression and expansion[a]

	ΔG_{com}	ΔG_{exp}	1st $\Delta\Delta G$	ΔG_{recom}	ΔG_{reexp}	2nd $\Delta\Delta G$
Lipid Fraction	+0.794	−0.509	+0.285	+0.649	−0.519	+0.130
Total Myelin	+1.068	−0.442	+0.626	+0.685	−0.448	+0.237

[a]The free energy of compression and expansion between the surface pressures of 2 and 42 mN/m (ΔG values expressed in Kcal/mol) are calculated from the areas under the surface pressure–area isotherms. $\Delta\Delta G$ is the difference between the ΔG_{com} and ΔG_{exp}. The first and second $\Delta\Delta G$ represent the free energy trapped in the monolayer during the first and second cycle of hysteresis, respectively, as shown in Fig. 4. Abbreviations; com: compression, exp: expansion, recom: recompression, reexp: reexpansion.

molecular energies) in a monolayer (Carrer and Maggio, unpublished results). In the first hysteresis cycle, $\Delta\Delta G$ for the whole myelin monolayer is more than twice the value obtained for the total lipid fraction (Table 2). Clearly, the total protein fraction adds a substantial element of structural asymmetry in the cohesive interactions of the interface.

Recompression of the films leads to considerable variation in the characteristics of the isotherm and in their hysteresis behavior (see Fig. 4), especially for the whole myelin monolayer. As shown in Table 2 the free energy taken up during recompression of the whole myelin monolayer is much smaller, and that of the lipid fraction is only moderately reduced (compared to that involved in the first compression), so that both become similar in the second cycle. The free energy released in the second expansion is essentially unaltered. This causes the $\Delta\Delta$G values of the second hysteresis cycle to become smaller and similar for both the myelin and lipid fraction than those found in the first cycle. These results emphasize the influence of total proteins in the initial behavior of the monolayer from whole myelin. A marked and irreversible intermolecular reorganization occurs during the first compression at a surface pressure of ca. 20 mN/m, that is mostly contributed by the protein fraction (and/or by its interaction with lipids).

If the compression of the whole myelin monolayer is carried out up to only 16 mN/m before expanding, little hysteresis and no major differences between the first and second cycles were observed (Fig. 5, compare also with Fig. 4(b)). If, after this, a third cycle of hysteresis is carried out by compressing the same myelin monolayer up to collapse (data not shown), then the surface behavior and the $\Delta\Delta G$ value are similar to the findings described in Fig. 4(b) and Table 2. This indicates that the protein fraction undergoes reorganization during the first compression, only if the surface pressure reaches values above 20 mN/m. The behavior of the myelin monolayer in the second compression becomes more similar to that of the lipid fraction, although still having a significantly different compressibility and magnitude of the surface potential/molecule (see below). This indicates that the protein components remain in a state of organization, different than the initial one, and in which they contribute very differently to the molecular packing and surface electrostatics. Calculation of the surface pressure–molecular area isotherm of the protein fraction under the expansion process (Fig. 6) reveals a rather incompressible isotherm in ranges of molecular area changes that are largely reduced compared to those obtained in the first compression. This also points to a considerable reorganization of the protein components in the myelin monolayer submitted to a first compression at > 20 mN/m.

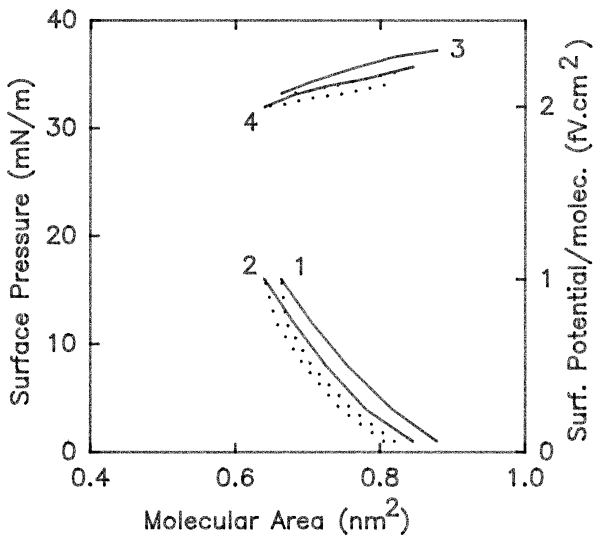

Fig. 5. Hysteresis of myelin monolayer compressed below 20 mN/m. Curve numbers as in Fig. 4. A third cycle of compression–expansion (not shown) carried out by compressing the film up to 40 mN/m after the second cycle gave a hysteresis behavior similar to that shown in Fig. 4(b) (see text).

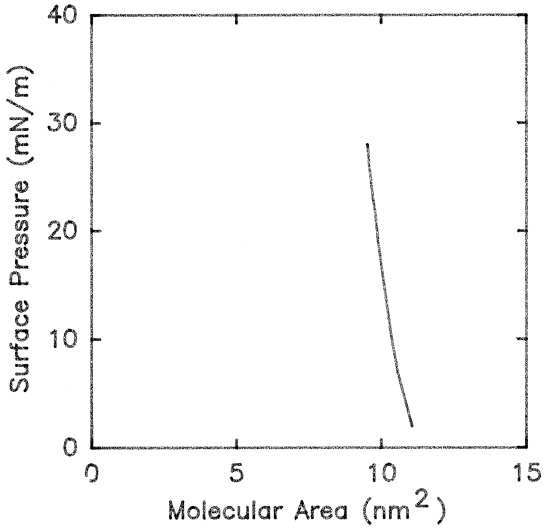

Fig. 6. Calculated isotherm of the protein fraction under expansion after the first compression up to above 30 mN/m.

Typical myelin proteins such as Folch–Lees proteolipid and myelin basic protein acquire a state of maximum close packing in pure protein monolayers at surface pressures between 12 and 20 mN/m [31,34,37] either by surface spreading or adsorption from the subphase. Moreover, the stability of protein molecules is increased and its molecular area further reduced if they are closely packed in mixed monolayers with lipids [31] in which the lipid–protein interactions also lead to a maximum compaction of the lipid cross-sectional area [38]. These previous observations in mixed monolayers of purified proteins and lipids of myelin, including myelin glycosphingolipids, and the hysteresis properties described in this work lend support to an interpretation based on a protein- and surface pressure-mediated reorganization of the myelin monolayer. This is reflected by the acquisition of an irreversible closely packed state of myelin, mediated by the protein components, when the interface is compressed above 20 mN/m, probably by facilitating close interaction with the lipid fraction. It has previously been shown that highly favorable interactions exist between myelin proteins and typical myelin lipids, leading to increased interfacial stability of both components, with reductions of the mean molecular area and surface potential/molecule [38]. On the other hand, proteins appear to contribute to an initial more expanded state of spread myelin before compressing it above 20 mN/m. Thus, it is tempting to speculate that myelin proteins may act as surface compensators for the transition between a liquid-expanded and a liquid-condensed state of myelin, depending on the lateral surface pressure: maintaining a liquid-expanded reversible state whenever the surface pressure fluctuates below 20 mN/m or facilitating an irreversible, liquid-condensed, closely packed state that can potentially acquire monolayer–multilayer equilibrium when the surface pressure exceeds 20 mN/m.

The hysteresis properties are also exhibited by the surface potential/molecule. These also indicate that the molecular reorganization of the monolayer occurring in the first compression is maintained and ''remembered'' when it is subsequently expanded. As shown in Fig. 4, during the first compression the overall resultant dipoles that determine the surface potential of the myelin monolayer and that of the total lipid fraction undergo increased reorientation and/or relocation beyond molecular packing areas of 0.62 nm^2 and 0.50 nm^2, respectively, corresponding for both films to a surface pressures of ca. 20 mN/m. Also, Fig. 4 shows that the dipolar reorganization occurring during the first expansion is much less than that observed during the first compression; no meaningful differences are introduced by further cycles of recompression–reexpansion. Fig. 4 shows that, in hysteresis cycles subsequent to the first, the variation of surface potential/molecule with the molecular area of the myelin monolayer becomes similar to that found for the total lipid fraction, although remaining with a considerable difference in magnitude due to the presence of the rearranged protein dipoles.

It is important to note that molecules are not desorbed from the interface during the hysteresis cycles. This is concluded from the similar limiting molecular areas obtained near collapse in successive cycles; also, the magnitude of the surface potential/molecule of the whole myelin monolayer after the second compression and thereafter stays considerably above that of the total lipid fraction; this indicates that the rearranged protein dipoles remain at the interface. Excellent reproducibility of the hysteresis cycles is obtained even if the monolayer was left for 10 min at 0.5 mN/m, before recompressing after the first expansion. No increase of surface pressure due to the well-known process of interfacial unfold-

ing of proteins is observed, even before the first compression, when the monolayer is left uncompressed for 30 min at the low pressure. This is different from the behavior of monolayers prepared from other cell membranes [18] and from that of axolemma monolayers that was reported previously [5]. With more simple binary lipid–protein mixtures, we have previously reported that interactions of several proteins, including myelin basic protein, with myelin lipids and glycolipids in monolayers resulted in a surface compaction and stabilization of the protein components in the mixed lipid–protein monolayer [31,38,39]. In axolemma, reproducible hysteresis cycles were found when the film was immediately compressed after expansion indicating that, different to myelin, the changes in molecular organization of the total protein fraction of axolemma are not stabilized by close packing with lipids. Furthermore, and again different to myelin, if the axolemma monolayer was left at pressures < 5 mN/m for more than 5 min, continuous increases of surface pressure due to protein unfolding were observed, after which the isotherms were no longer reproducible [5].

4. Conclusions

In this work, we have achieved for the first time the formation of a monomolecular layer from the myelin membrane. It has thus been possible to have measurements of the mean molecular packing area, surface electrostatics, and compressibility properties of myelin and of its major lipid and protein fractions under well-defined compression and expansion conditions.

Taken together (the initial compression isotherm of the whole myelin monolayer, that of the total lipid fraction, the compression isotherm of the total protein fraction, the features of the second compression of the myelin monolayer, and the expansion isotherm of the total protein fraction), our results indicate that the marked reorganization of the myelin membrane occurring > 20 mN/m is not reversible and is mostly due to the protein fraction. Our observations indicate that myelin can form a remarkably stable interface at high surface pressures (i.e. > 30–35 mN/m, such as those present in cell membranes [40]) and that it can acquire under compression (or spontaneously by adsorption) a state of equilibrium between a closely packed, organized monolayer and a bulk (multilayered) structure. Spontaneous bilayer and multilayer formation at the air–water interface was reported in pure lipid systems and in complex lipid mixtures [41]. The behavior found herein for the myelin monolayer provides a physico-chemical basis for the spontaneous formation and maintenance of a remarkably stable multilayered biological structure of myelin.

Acknowledgements

This work was supported in part by SECyT-UNC, CONICOR, CONICET and Fundación Antorchas, Argentina. Rafael G. Oliveira is a Fellow and Bruno Maggio is Principal Career Investigator from CONICET. Reyna O. Calderón is currently Assistant Professor at the 1a. Cátedra de Embriología, Histología y Genética, Facultad de Ciencias Médicas, Universidad Nacional de Córdoba, Argentina.

References

[1] K.S. Birdi, Lipid and Biopolymers Monolayers at Liquid Interfaces, Plenum Press, New York, 1989.
[2] B. Maggio, Prog. Biophys. Molec. Biol. 62 (1994) 55–117.
[3] R. Verger, F. Pattus, Chem. Phys. Lipids 16 (1976) 285–291.
[4] F. Pattus, C. Rothen, M. Streit, P. Zahler, Biochim. Biophys. Acta 647 (1981) 29–39.
[5] O.R. Calderón, B. Maggio, T.J. Neuberger, G.H. DeVries, J. Neurosci. Res. 34 (1993) 206–218.
[6] O.R. Calderón, B. Maggio, T.J. Neuberger, G.H. DeVries, J. Neurosci. Res. 40 (1995) 349–358.
[7] J.E. Haley, F.G. Samuels, R.W. Leeden, Cel. Mol. Neurobiol. 1 (1981) 175–178.
[8] C. Wutrich, A.J. Steck, Biochim. Biophys. Acta 640 (1981) 195–206.
[9] B. Maggio, R.K. Yu, Biochim. Biophys. Acta 1112 (1992) 105–114.
[10] B. Maggio, F.A. Cumar, Brain Res. 77 (1974) 297–307.
[11] G.R. Barlett, J. Biol. Chem. 234 (1959) 466–468.
[12] T. Coetzee, N. Fujita, J. Dupree, R. Shi, A. Blight, K. Suzuki, R. Suzuki, B. Popko, Cell 86 (1996) 209–219.
[13] L.J. Macala, R.K. Yu, S. Ando, J. Lipid Res. 24 (1983) 1243–1250.
[14] U.K. Laemmli, Nature 227 (1970) 680–685.
[15] J.H. Morrisey, Anal. Biochem. 117 (1981) 307–310.
[16] O.H. Lowry, N.J. Rosebrough, A.L. Farr, R.J. Randall, J. Biol. Chem. 193 (1951) 265–275.

[17] B. Maggio, T. Ariga, R.K. Yu, Biochem. 29 (1990) 8729–8734.
[18] Th. Schurholz, H. Schindler, Eur. J. Biophys. 20 (1991) 71–78.
[19] I.D. Bianco, G.D. Fidelio, R.K. Yu, B. Maggio, Biochem. 30 (1991) 1709–1714.
[20] G.L. Gaines, in: I. Prigogine (Ed.), Insoluble Monolayers at Liquid-Gas Interfaces, Interscience Monographs on Physical Chemistry, John Wiley and Sons, New York, 1996.
[21] B. Maggio, F.A. Cumar, R. Caputto, Biochem. J. 171 (1978) 559–565.
[22] B. Maggio, in: M.J. Allen, S.F. Cleary, A.E. Sowers, F.M. Hawkridge (Eds.), Charge and Field Effect in Biosystems-III, Birkhauser, Boston, 1992, pp. 69–80.
[23] K.E. VanHolde, Physical Biochemistry, 2nd ed., Prentice Hall Inc., Englewood Cliffs, New Jersey, 1985.
[24] P. Morell, R.C. Wiggins, M.J. Gray, Anal. Biochem. 68 (1975) 148–154.
[25] D.F. Sears, R.E. Stark, in: L.M. Prince, D.F. Sears (Eds.), Biological Horizons in Surface Science, Acad. Press, New York, 1973, pp. 1–33.
[26] K. Larsson, in: F.D. Gunstone, J.L. Harwood, F.B. Padley (Eds.), The Lipid Handbook, 2nd ed., Chapman and Hall, London, 1994, pp. 419–422.
[27] D. Chapman, Quart. Rev. Biophys. 8 (1975) 185–235.
[28] A. Mattus, S. de Petris, M.C. Raff, Nature New Biol. 244 (1973) 278–280.
[29] L.A. Autilio, W.T. Norton, R.D. Terry, J. Neurochem. 11 (1964) 17–27.
[30] F. Gonzales-Sastre, J. Neurochem. 17 (1970) 1049–1056.
[31] G.D. Fidelio, B. Maggio, F.A. Cumar, An. Asoc. Quim. Argen. 74 (1986) 801–813.
[32] K. Nag, J. Perez-Gil, A. Cruz, N.H. Rich, M.W. Keough, Biophys. J. 71 (1996) 1356–1363.
[33] F. MacRichtie, Adv. Protein Chem. 32 (1978) 283–326.
[34] Y. London, R.A. Demel, W.S.H. Geurts van Kessel, F.G.A. Vossemberg, L.L.M. van Deenen, Biochim. Biophys. Acta 311 (1973) 520–530.
[35] M. Galdston, D.O. Shah, Biochim. Biophys. Acta 137 (1967) 255–263.
[36] D. Lusted, Biochim. Biophys. Acta 307 (1973) 270–278.
[37] G. Colacicco, Ann. N.Y. Acad. Sci. 195 (1972) 224–261.
[38] G.D. Fidelio, B. Maggio, F.A. Cumar, Chem. Phys. Lipids 35 (1984) 231–245.
[39] B. Maggio, Neurochem. Res. 22 (1997) 475–481.
[40] D. Marsh, Biochim. Biophys. Acta 1286 (1996) 183–223.
[41] N.L. Gershfeld, Biochim. Biophys. Acta 988 (1989) 335–350.